International Journal of Multidisciplinary Research and Development
Online ISSN: 2349-4182, Print ISSN: 2349-5979; Impact Factor: RJIF 5.72
Received: 21-04-2020; Accepted: 23-04-2020; Published: 01-05-2020
www.allsubjectjournal.com
Volume 7; Issue 5; 2020; Page No. 12-17

Physico-chemical and spectroscopic properties of two laterite soils for applications in arsenic water treatment

Yacouba Sanou[1*], Clement Kolawole Balogoun[2], Rasmane Tiendrebeogo[3], Raymond Kabore[4], Ibrahim Tchakala[5], Samuel Pare[6]

[1, 3, 4, 6] Laboratory of Analytical, Environmental and Bio-Organic Chemistry, UFR/SEA, University Joseph KI-ZERBO, 03 BP 7021 Ouagadougou 03, Burkina Faso

[2] Applied Chemistry Study and Research Laboratory, Polytechnic School of Abomey-Calavi University, 01 BP. 2009, Benin

[5] Laboratory of Applied Hydrology and Environment, Faculty of Sciences, University of Lomé, BP. 1515, Togo

Abstract
Access to safe drinking water constitutes a challenge for some rural areas in Burkina Faso where groundwater, unique source of domestic water supply, is contaminated by arsenic. Natural laterite (NL) and thermal treated laterite (TL) at 400°C were prepared and used as adsorbent for arsenic removal from enriched groundwater. The prepared adsorbents were characterized by spectroscopic techniques such as X-rays diffraction, energy dispersive spectroscopy, Fourier transform-Infrared, Brunauer-Emmett-Teller analysis, scanning electron microscopy and physical methods. Those prepared adsorbents contain aluminum oxide, quartz, hematite and goethite as mineral phases. The thermal treatment induces higher surface area of TL vs NL. Studied groundwater sample contained arsenic concentration of 122 µg/L, as well as anionic compounds such as bicarbonates, sulfates, phosphates and chlorides which can compete with arsenic removal. The treatment of arsenic water using column experiments was influenced by the flow rate of water and it became less efficient when the flow rate increased. Better treatment of arsenic (305 µg As /g for NL and 402 µg/g for TL under operational conditions) was achieved at flow rate of 8 mL/min for TL and 4.5 mL/min using NL.

Keywords: arsenic, characterization, laterite, soil use, water treatment

1. Introduction
Drinking water supply is one of the most important challenges of African countries, mainly in Sub-Sahara Africa. Arsenic contamination in groundwater for drinking purposes has become a worldwide problem and a serious environmental challenge in the world [1-3]. Several technologies have been developed for the treatment of water including adsorption and filtering methods [4-6]. Among them, adsorption is one of the most popular processes in arsenic removal from water because of its cost-effective, high affinity for dissolved arsenic and it doesn't produce sludge [7]. Most of the studies on arsenic removal have been conducted in batch operation [8]. Its implementation in continuous column experiments can be used in small scale household units. Some works on column studies have been reported in literature [9-13]. So far, various adsorbents either from natural and synthetic origin have been investigated for arsenic removal. Development and implementation of cheap natural adsorbents such as activated carbons, clay, ferric hydroxide, laterite, and active silica were successfully used to remove arsenic from water [9, 10, 14]. In general, commercial adsorbents including carbons, granular ferric hydroxide, and others are described as limited in their use due to high operational cost [15]. For this reason, other economic and eco-friendly materials for water purification were looked for. A preliminary study using laterite indicated that its adsorption capacity was low compared to granular ferric hydroxide and activated carbons [16]. The use of laterite soils for depollution purpose requires the determination of its surface morphology, microstructure, chemical composition, chemical surface functions and surface area which were not determined. The present work aims to make a comparative study of properties of natural laterite and thermally treated laterite in order to their use as fixed bed in column experiments for arsenic removal. In this study, we investigated the properties and characteristics of natural laterite (NL) and treated laterite (TL) using spectroscopic methods.

2. Material and methods
2.1. Collection and preparation of natural laterite (NL) and treated laterite (TL)
Laterite used in this work was collected in Balkuy district (12°17'23''N, 1°27'47''W), one of the peripheral districts of Ouagadougou (Burkina Faso). Raw laterite was sampled and sent to the SGS mineral laboratory for crushing and washing using the protocol described as follow. The natural laterite (NL) was crushed with hammer, washed thoroughly with distilled water and then dried in an oven (Interlabs DP1-I Instruments) at 105 ° C for 24 h. Then, it was crushed and sieved (AFNOR sieve) to retain particles of sizes comprised between 1.5 and 2.5 mm.
The treated laterite (TL) has been prepared according to a method previously described [4, 17]. Raw laterite was thermally calcined at 400°C for 4 hours in an oven (Prolabo VOLCA, MC25) with a rise speed of 10°C /min. The calcined laterite was crushed again and sieved using two screens with 1.5- and 2.5-mm pore sizes. TL grains were washed with distilled water and then dried at 120°C for 6 hours in an oven.

2.2. Characterization techniques of NL and TL

2.2.1. Spectroscopic methods

Energy Dispersive Spectroscopy (EDS) was used to determine the chemical composition of NL and TL. The surface morphologies of laterite soils were analyzed with Scanning Electron Microscopy (SEM) using a "JED-2300, 7410F" microscope coupled to an EDS detector. Fourier Transform-Infrared spectrum of laterite soil was recorded to detect the surface functional groups using an infrared spectrophotometer (TENSOR 27 - BRUKER - GERMANY) operating in the range of 4000 - 400 cm^{-1} and using potassium bromate pellet (KBr). X-rays diffraction of NL and TL was carried out using a diffractometer (Philips, PW-1130) with the monochromatic radiation $K\alpha_1$ of Copper (1.5406 Å). The constant S/R indicating the classification of laterite soils have been calculated using following equations [18]:

$$\frac{S}{R} = \frac{\frac{SiO_2}{60}}{\frac{Al_2O_3}{102} + \frac{Fe_2O_3}{160}} \quad (1)$$

2.2.2. Determination of the surface area

The Brunauer-Emmet-Teller (BET) method was used to determine the specific surface of natural laterite and treated laterite. This measurement is carried out at 77 K using an analyzer "Micrometics, ASAP 2024" device with a liquid nitrogen as adsorption gas.

2.2.3. Determination of bulk density

It is a physical parameter used to estimate the mineralogical composition of raw materials. The density is calculated according to the following equation:

$$\rho = \frac{m_1 - m_0}{V} \quad (2)$$

With m_0 is the mass of the empty conical flask, m_1: mass of the flask filled with laterite. V: volume of the empty flask.

2.2.4. Determination of pH at zero-point charge

The pH at zero-point charge noted pH_{ZPC} is the pH for which the overall electrical charge of the adsorbent is neutral and corresponds to the isoelectric pH of the material. It is determined according to the method described by Noh *et al.* [19].

2.3. Contaminated water sampling site

The sampling was done at Mogtédo village (12°17'4''N, 0°49'45''W) located 82 km from Ouagadougou. This borehole water is the source of drinking water supply for the Mogtedo municipality. Excepted chlorine disinfestation, no additional depollution treatment is carried out before the distribution of water. Mogtedo is an area with mining, gold in particular and many cases of arsenic contamination and high concentrations in boreholes have been reported in previous works [20, 21].

2.4. Sampling and characterization of water samples

Groundwater samples were collected on November 2018. Water box (drums) with a volume of 20 liters previously cleaned with 10% HNO_3 solution and rinsed with distilled water was used. Five (05) physico-chemical parameters (pH, temperature, turbidity, electrical conductivity (EC) and arsenic concentration) were measured in situ. Temperature and pH were measured with a pH-meter (Electrode martini, Mi 606). Electric conductivity and turbidity were analyzed with Conductimeter (Thermo Scientific, orient 3STAR) and Turbidimeter Wagtech, respectively. Arsenic concentration was measured in-situ with an Arsenator Palintest.

In the Laboratory, the phsico-chemical composition of groundwater sample was determined. Total Hardness (TH), Total Alkalinity (TAC), Total Suspended Solids (TSS) were determined according to APHA standard methods [24]. Anionic species such as phosphate, bicarbonate, sulfate, chloride, nitrate and fluoride were determined using colorimetric methods with an Ultraviolet-Visible Spectrophotometer (Hach Lange, DR 3900). Arsenic concentration was determined using Inductively Coupled Plasma - Atomic Emission Spectroscopy (ICP-AES).

2.5. Arsenic removal tests: column experiments

Experiments were carried out with a pilot using the PVC column (height 150 cm and diameter 9 cm). The setting up of the column includes glass wools and glass beads with adsorbent (NL and TL).The operating principle consists in passing the contaminated water from the bottom to the top (up flow) in the column filled with known laterite mass in order to follow the arsenic concentration and the turbidity of the effluent at the column outlet vs time.

The percentage of arsenic removal (As Removal) is calculated by the following relation:

$$As\ Removal = \frac{C_0 - C_t}{C_0} \times 100 \quad (3)$$

C_0 and C_t represent arsenic concentration (µg/L) in influent and effluent water, respectively.

3. Results and discussion

3.1. Microstructure of NL and TL

SEM images at 5000 magnifications are presented in Figure 1. While the figure 2 shows the SEM micrographs of at 10000 magnifications. Analysis of figure *1a* shows the presence of the clusters distributed over each in the form of platelets as well as the existence of pores within the laterite. In Fig. *1b*, a more compact and rougher surface is noted, with large pores, indicating possible greater specific surface. The platelets (figure 1) of goethite or hematite and other minerals have a rather irregular, disordered morphology, without any particular shape, do not allow them to be distinguished. The Fig. *2a* shows most likely regular macropores of NL while stacks of likely hexagonal platelets and the fine pores are observed in Fig. *2b*. The stacks and fine pores (Fig. 2) contribute to increase of the specific surface of TL vs NL. The surface appears shiny in places which could reflect iron oxides on the surface or an inhomogeneous distribution of the iron atoms in the sample.

Figure 1: SEM images of NL and TL magnified 5000 times

Figure 2: SEM images of NL and TL at 10000 magnifications

3.2. Chemical and elemental composition of NL and TL

EDS spectra of NL and TL are presented in Figure 3 indicating the basic surface analysis of the adsorbents. The EDS spectrum of NL (Fig. 3a) showed the presence of chemical elements such as silicon, aluminum, iron, oxygen and carbon at different percentages. In addition of those elements identified in Fig. *3a*, there is magnesium in Fig. *3b*

for TL. The amount of the chemical elements are given in Table 1.

a. Natural Laterite
b. Treated Laterite

Figure 3: EDS spectra of NL and TL acquired under 20 keV

Chemical composition of soils including the elemental and qualitative compositions which indicate the chemical elements and their possible oxides in NL and TL is given in Table 1. Results revealed important percentage of oxides of silicon, aluminum and iron. An increase of the content of silicon, aluminum, oxygen and carbon in TL vs NL is observed, as a possible consequence of the thermal treatment which increases or improves the properties of laterite. In addition, there is a mixture of oxide which could contain magnesium, calcium, and copper which are not detected on EDS spectra in previous works [4, 14]. Excepted Fe_2O_3, the amount of detected oxides increased after the thermal treatment (TL). The lower content of iron oxide in laterite soils compared to those of aluminum and silicon could justify its low adsorption capacity of arsenic previously revealed [4, 23]. These chemical elements identified are those commonly encountered in previous study [4]. The constant S/R =1.23 for NL is less than 1.33 indicating that NL would be a true laterite and its increase in TL could be explained by the thermal treatment which increased the content of quartz from 37.02 to 44.69% [17, 18].

Table 1: Elemental chemical composition of NL and TL (m/m)

3.3. Surface functional groups of laterites

Figure 4 represents the infrared spectrum of NL, which is analyzed with literature data [4, 14, 24]. This spectrum identifies the probable chemical functions on the surface of NL. The bands at 3693 and 3620 cm^{-1} are attributable to the vibrations of the external and internal hydroxyls Al-OH, respectively [24]. The band around 3161 cm^{-1} corresponds to the vibration of the -OH bond of iron oxy-hydroxides [4, 14]. The band at 1633 cm^{-1} is assigned to hydroxyls of water molecules between the layers. The band around 1033 cm^{-1} is attributable to the vibration of the Mg-O bond and the band around 913 cm^{-1} corresponds to the vibration of the Al-OH bond [14, 24]. The band at 795 cm^{-1} is attributable to the vibration-bending of the Fe-OH bond [24]. The double band at 539 and 463 cm^{-1} indicates the presence of the Si-O-Si or Si-O-Al group [4, 14].

Figure 4: Infrared spectrum of NL recorded between 400 and 4000 cm^{-1}

3.4. Qualitative composition of NL and TL

X-ray diffractogram (Figure 5) shows the qualitative composition of laterites composed of quartz, alumina, hematite, goethtite, tenorite, periclase and lime.

Figure 5: X-rays diffractogram of TL

Data in Table 2 revealed that the laterite soils were essentially composed of quartz, alumina, hematite, and goethite with a predominance of quartz and alumina. An increase of the amount of quartz and alumina in mineral phases due to the effect of thermal treatment was noted while the amount of other mineral phases decreased. The mixed oxides in Table 1 could contain tenorite, lime and periclase at low amount. All these crystalline phases are currently present in natural laterite soils [25]. The presence of mineral adsorbents (Fe and Al oxides) could contribute to increase the adsorption capacity of TL comparatively to NL [16]. These mineral phases observed in TL are in agreement with those found mainly by Krishna *et al.* [26].

Tableau 2: Qualitative composition of NL and TL

3.5. Physico-chemical characteristics of NL and TL

BET multipoint graph allowed to determine the specific surface of laterite (Fig. 6). Surface areas of NL and TL were 42.39 m^2/g and 52.47 m^2/g, respectively. The surface area of TL is higher than the one of NL. The significant increase in the specific surface area of calcined laterite could be explained by the transformation of iron oxides under the action of activation. This would promote the formation of new pores on the surface as shown by SEM images and thus contribute to the increase of the specific surface. As adsorption occurring on surface, increasing the specific surface could contribute to increasing the adsorption capacity of the material.

Figure 6: BET multipoint Graph of NL and TL

At zero point of zero, natural laterite has a pH of 7.91 compared to pH_{ZPC} of TL that is 5.74. The pH_{ZPC} of NL is included in the range of pH_{ZPC} (6.96 - 8.64) found in the literature for natural laterites [4, 17]. The decrease of pH during the thermal treatment (TL) could be explained by deshydroxilation and decarbonization under the effect of temperature. In addition, the decease of pH after thermal treatment could be due to quartz having an acid property.

Natural Laterite has a bulk density of 2.53 g/mL and this value is closed to the value reported earlier [4]. The density of TL is 2.45 g/mL, this value lower than that of NL measured under the same conditions. This result is in agreement with previous study which indicates that thermal treatments cause the induration of laterite by increasing its density [27].

In order to evaluate the possible efficiency of two prepared and characterized laterite soils for arsenic water treatment, natural groundwater collected in Mogtedo village was used.

3.6. Physico-chemical characteristics of water

Physico-chemical characteristics are presented in Table 3. It was observed that water contains an average of 122 µg / L of arsenic, which is 12 times the WHO value (10 µg/L). It contains a significant quantity of anions such as Cl^-, PO_4^{3-}, NO_3^- and HCO_3^- which can affect the adsorption of arsenic on laterite [4, 28-30].

Table 3: Physico-chemical parameters of groundwater

3.7. Arsenic water treatment

Five values of flow rate varying between 2 L/min, and 35.5 L/min were used with water containing an arsenic concentration of 122 µg/L in order to study the process performance after a treated water volume of 100 L for each flow rate. Results show a decrease of arsenic removal percentage when the flow rate increased (figure 7). Using NL, it was noted an arsenic removal percentage of 100% when the flow rate varied between 2 and 4.5 L/min. When the flow rate increased beyond 4.5 mL/min, arsenic removal decreased significantly until 65.5%. The decrease of arsenic removal when the flow rate increases can be explained by the shortcoming of contact time between arsenic ions and activated sites on the NL surface [4]. Better arsenic removal at low flow rate is in agreement with previous works indicating the moving and fixation of arsenic species on the surface of laterite [14, 31].

Unlike to NL, the influence of the flow rate on arsenic removal using TL was evaluated between 6.5 and 37.5 mL/min (Figure 7). Obtained results show the decrease of arsenic removal from 100% to 81.15% when the flow rate increased from 6.5 to 37.5 mL/min. Between the flow rates of 6.5 and 8.5 mL/min, better arsenic removal yield of 100% was achieved after 45 min of treatment. When the flow rate was increased up to 34.5 mL/min in order to produce a lot of drinking water, it was noted a decrease of arsenic removal from 100% to 79%. The decrease in removal yield using TL could be due to the decrease of contact time for the fixation of arsenic ions onto the pores of TL. This result may be due to the decrease of empty bed contact time in the column for the electrostatic fixation of arsenate and arsenite on the activated sites of TL.

Using the same flow rate, TL presents a high removal capacity compared to the one of NL. Indeed, using a flow rate of 8.5 mL/min, NL removed 90.5 % of arsenic while TL removed 100% of arsenic indicating the high performance of TL. High efficiency of TL vs NL in the same experimental conditions could be explained by the improvement of TL properties using the thermal treatment.

Figure 7: Effect of flow rate on arsenic removal using NL and TL with m = 40 g, pH = 7.04, C_0 = 122µg/L, and T = 25 ± 2°C.

Table 1: Elemental chemical composition of NL and TL (m/m)

Elemental composition (%)	Si	Al	O	Fe	C	Mixture (Mg, Ca, Cu)
NL	18.27	17.39	41.39	20.38	1.06	1.51
TL	21.28	20.89	45.94	8.71	1.9	1.28
Oxides (%)	SiO_2	Al_2O_3	Fe_2O_3	$\frac{S}{R}$	Mixed oxides (CuO, MgO, CaO)	
NL	37.02	34.52	26.22	1.23	2.24	
TL	44.69	40.20	11.21	1.6	3.1	

Table 2: Qualitative composition of NL and TL

Mineral phases % (m/m)	Quartz	Alumina	Hematite	Goethite	Tenorite	Periclase	Lime
NL	47.43	30.5	10.87	4.35	1.31	3.10	2.47
TL	52.1	33.4	7.85	3.3	0.32	1.45	1.33

Table 3: Physical-chemical parameters of groundwater

Parameter	T (°C)	pH	EC (µS/cm)	Turbidity (NTU)	TSS (mg/L)	TH (°F)	TA (mg/L)	DS (mg/L)	TS (mg/L)
Value	33.30	6.96	495	0	21	7.97	11.32	305	326
WHO limit	25	6.5-8	300	≤ 5	26	7-15	*	*	*
Parameter	Total As (µg/L)	HCO_3^-(mg/L)	NO_3^-(mg/L)	F^-(mg/L)	Cl^-(mg/L)	PO_4^{3-}(mg/L)	SO_4^{2-}(mg/L)	Ca^{2+} (mg/L)	Mg^{2+} (mg/L)
Value	122	6.5	6.3	< LD	109	1.26	< LD	14.03	11.57
WHO's value	10	*	50	1.5	50	*	*	200	50

(*): value not found (not available) LD: limit of detection

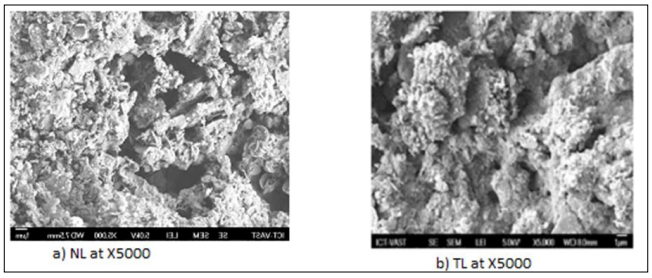

Fig 1: SEM images of NL and TL magnified 5000 times

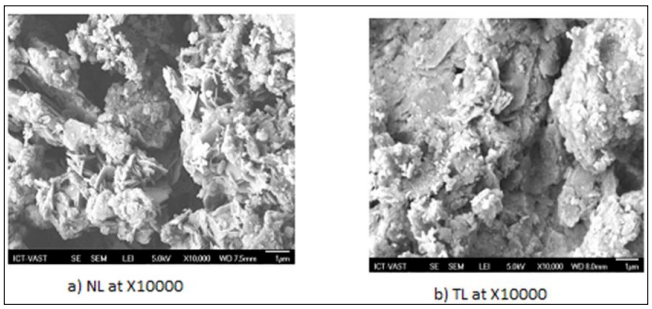

Fig 2: SEM images of NL and TL at 10000 magnifications

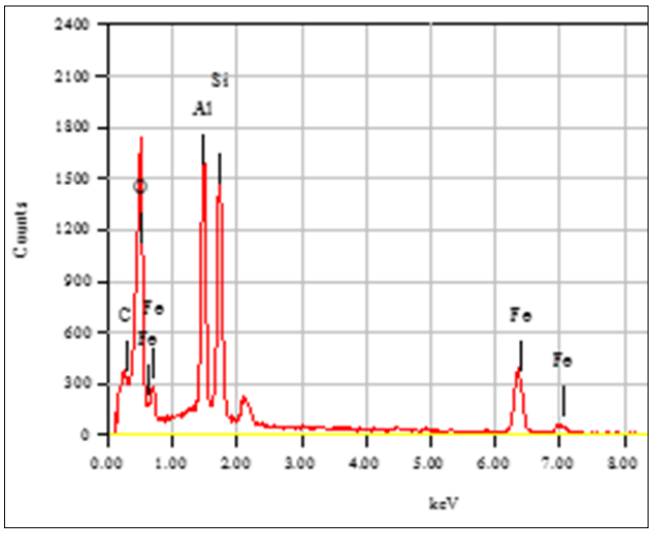

Fig 3a: EDS spectra of NL acquired under 20 keV

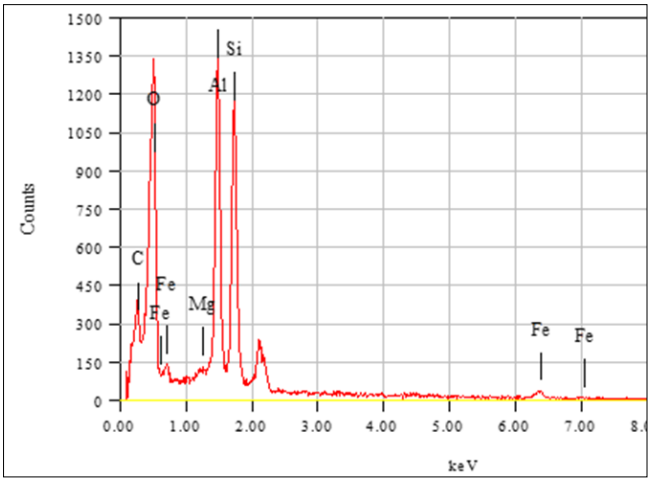

Fig 3b: EDS spectra of TL acquired under 20 keV

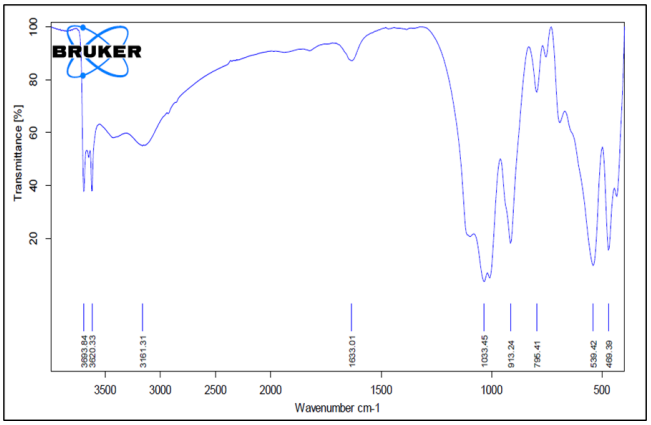

Fig 4: Infrared spectrum of NL recorded between 400 and 4000 cm^{-1}

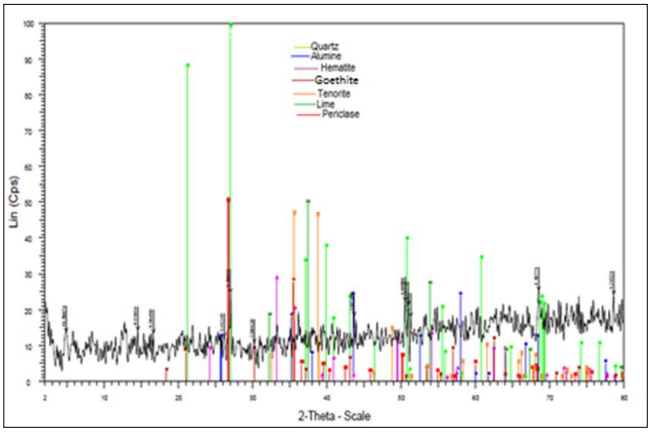

Fig 5: X-rays diffractogram of TL

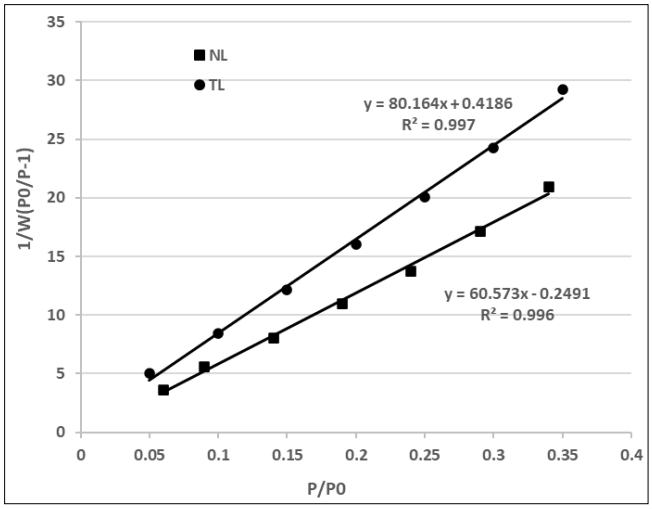

Fig 6: BET multipoint Graph of NL and TL

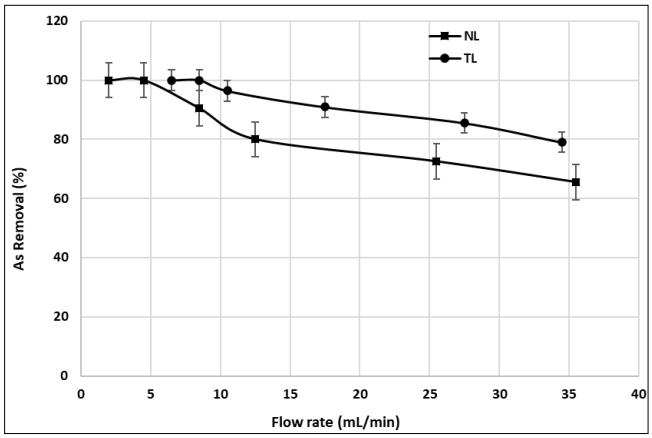

Fig 7: Effect of flow rate on arsenic removal using NL and TL with m = 40 g, pH = 7.04, C_0 = 122µg/L, and T = 25 ± 2°C.

4. Conclusions

The surface area of natural laterite and treated laterite were 42.39 and 52.47 m^2/g, respectively. Bulk density of NL was 2.53 g/mL comparatively to 2.45 g/mL for TL. At zero-point charge, pH of NL was 7.91 while TL had a pH of 5.74. Analysis using EDS showed the presence of silicon, aluminum, carbon, oxygen, and iron incorporated in the structure of NL and TL with high oxygen content. XRD spectra revealed the presence of iron oxides, aluminum oxide, lime, tenorite and others. Those compounds are in agreement with IR spectra which indicated some metallic oxides/hydroxides as functional groups on the surface of NL. The process of arsenic removal was influenced by the flow rate of water and the treatment of arsenic water becomes less efficient when the flow rate increased. Total treatment of arsenic (100% of removal) was noted at flow rate less than 8 mL/min indicating an adsorption capacity of 305 µg/g. At this regard, laterite soils (NL or TL) should be a hopeful adsorbent for the treatment of arsenic water using continuous experiments. That will contribute to decrease the water diseases such as melanosis, hyperkeratosis and skin changes due to arsenic contamination

Acknowledgement

This research did not receive any specific grant or financial support from funding agencies in the public, commercial, or not-for-profit sectors. The authors declare that there is no conflict of interests regarding the publication of this paper.

Authors thank to Vietnamese Academy of Sciences and Technology for their technical support.

References

1. Jain CK, Ali I. Arsenic: Occurrence, toxicity and speciation techniques. Water Research. 2000; 8:4304-4312.
2. Smedley PL, Kinniburgh DG. A review of the source, behavior and distribution of arsenic in natural water. Appl. Geochem. 2002; 17:517-568.
3. Hughes MF. Arsenic toxicity and potential mechanisms of action. Toxicology Letters. 2002; 133:1-16.
4. Sanou Y. Traitement des eaux avec des charbons actifs, GFH et latérite. Editions Universitaires Européennes, tvisrasco, 2019, 1-157.
5. Mahvi AH, Naghipour D, Vaezi F, Nazmara S. Tea waste as an adsorbent for heavy metal removal from industrial wastewaters. Am. J Appl. Sci. 2005; 2:372-375.
6. Burggraaf AJ, Cot L. Fundamentals of inorganic membrane science and technology. Membrane Sci. Technol. Elsevier series. 1996; 4:67-118.
7. Tuna AOA, Ozdemir E, Simsek BE, Beker U. Removal of As (V) from aqueous solution by activated carbon-based hybrid adsorbents: Impact of experimental conditions. Chem. Eng. J. 2013; 223:116-128.
8. Sanou Y, Nguyen PTT, Pare S, Nguyen PV. The removal of As (V) from aqueous solutions using Ferromagnetic Activated Carbon: equilibrium and kinetic studies. Rev. Sci. Eau. 2019; 32(2):179-192.
9. Kundu S, Gupta AK. Analysis and modeling of fixed bed column operations on As (V) adsorption onto iron oxide-coated cement (IOCC). J Coll. Interf. Sci. 2005; 290:52-60.
10. Maji SK, Pal A, Pal T, Adak A. Modeling and fixed bed column adsorption of As (V) on laterite soil. J Environ. Sci. Health. 2007; Part A. 42: 1-95.
11. Roy P, Mondal NK, Bhattacharya S, Das B, Das K. Removal of arsenic (III) and arsenic (V) on chemically modified low-cost adsorbent: batch and column operations. J Appl. Water Sci. 2013; 3(1):293-309.
12. Gupta VK, Saini VK, Jain N. Adsorption of As (III) from aqueous solutions by iron oxide-coated sand. J. Coll. Interf. Sci. 2005; 288:55-60.
13. Kundu S, Kavalakatt SS, Pal A, Ghosh SK, Mandal M, Pal T. Removal of arsenic using hardened paste of Portland cement: batch adsorption and column study. Water Res. 2004; 38:3780-3790.
14. Sanou Y, Pare S, Nguyen PTT, Nguyen PV. Experimental and kinetic modeling of As (V) adsorption on Granular Ferric Hydroxide and laterite. J. Environ. Treat. Tech. 2016; 4(3):62-70.
15. Sanou Y, Mande Alfa-Sika SL, Vunain E, Pare S. Preparation and Characterization of Husk Based Carbons: Effect of the Temperature. J Environ. Treat. Tech. 2019; 7(1):150-157.
16. Sanou Y, Pare S, Arsenic pollution through drinking groundwater in Burkina Faso: research of a cheap removal technology, in: M. Nolasco, E. Carissimi, E. Urquieta-Gonzalez (Eds.) water perspectives in emerging countries: linking water security to sustainable development goals. Cuvillier Verlag Göttingen, Inc., Germany, 2018, 137-148.
17. Maiti A, DasGupta S, Basu JK, De S. Adsorption of arsenite using natural laterite as adsorbent. Sep. Pur. Technol. 2007; 55:350-359.
18. Martin JF, Dyne JC. Laterite and lateritic soils in Sierra Leone. J Agri. Sci. 1927; 17(04):530-547.
19. Noh JS, Schwarz JA. Estimation of the point of zero charge of simple oxides by mass titration. J coll. Interf. Sci. 1989; 130:157-164.
20. De Jong SJ, Kikietta A. Une particularité bien localisée, heureusement présence d'arsenic en concentration toxique dans un village près de Mogtédo (Haute-Volta). Bull. L. Com. Interafr. Et. Hydr, 1980, 44. 10.0.0.16/doc_pdf/bulletin-liaison_n°42-43.pdf.
21. Smedley PL, Knudsen J, Maiga D. Arsenic in groundwater from mineralized Proterozoic basement rocks of Burkina Faso. Appl. Geochem. 2007; 22:1074-1092.
22. Rice EW, Baird RB, Eaton AD, Clesceri LS. Standard methods for the examination of water and wastewater. American Public Health Association APHA, AWWA, WEF. 22th Edition, Washington DC, 2012, 2001- 3710.
23. Maiti A, Bassu JK, De S. Development of a Treated Laterite for Arsenic Adsorption: Effects of Treatment Parameters. Ind. Eng. Chem. Res. 2010; 49:4873-4886.
24. Millogo Y. Etude géotechnique, chimique et minéralogique de matières premières argileuse et latéritique du Burkina Faso améliorées aux liants hydrauliques: application au génie civil (bâtiment et route). Thèse de doctorat Unique, Université de Ouagadougou, 2008, 22-23.
25. Messeaouda S. Etude de la capacité de rétention et d'élimination des cations métalliques par des adsorbants naturels. Thèse unique, Université de Mustapha Stambouli, Mascara, Algérie, 2016.
26. Suresh Krishna M, Jeykumar RKC. Preparation of Amino-Modified Iron Oxide Nano Adsorbent and Calcined Laterite for Chromium (VI) and Copper (II) Removal. Inter. J. Biotech. Trends Technol. 2018; 8(2):18-20.
27. Bandyayera D. Formation des latérites nickélifères et mode de distribution des éléments du groupe du platine dans les profils latéritiques du complexe de Musongati au Burundi. Thèse de doctorat unique, Université du Québec, Canada, 1997, 1-495.
28. Gupta A, Sankararamakrishnan N. Column studies on the evaluation of novel spacer granules for the removal of arsenite and arsenate from contaminated water. Biores. Technol. 2010; 101(7):2173-2179.
29. Mälher J, Persson I. Rapid adsorption of arsenic form aqueous solutions by ferrihydrite-coated sand and Granular Ferric Hydroxide. Appl. Geochem. 2013; 37:179-189.
30. Driehaus W, Jekel M, Hildebrandt U. Granular ferric hydroxide: a new adsorbent for the removal of arsenic from natural water. J Water Supply: Res. Technol. Aqua. 1998; 47:30-35.
31. Ouvrard S. Couplage matériau / procédé d'adsorption pour l'élimination sélective d'arsenic présent en traces dans les eaux. Thèse de doctorat unique, Institut National Polytechnique de Lorraine, France, 2001, 1-222.